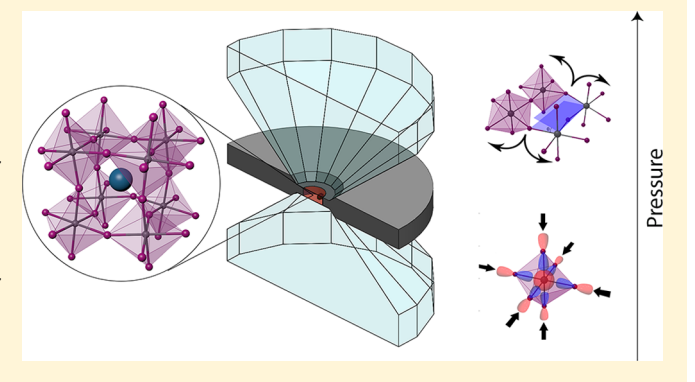
Pressure Response of Photoluminescence in Cesium Lead Iodide **Perovskite Nanocrystals**

J. Curtis Beimborn II,^{†,‡} Leah M. G. Hall,[‡] Pornthip Tongying,^{‡,§} Gordana Dukovic,[‡] and J. Mathias Weber*,†,‡®

ABSTRACT: In this paper, we address the phase stability and the relationship between optical gap and structural perturbations in cesium lead halide nanocrystals. We report photoluminescence (PL) spectra for cesium lead iodide (CsPbI₃) perovskite nanocrystals under hydrostatic pressures up to 2.5 GPa. The peak position of the CsPbI₃ PL shifts as a function of pressure. Initially, the PL shifts to lower energies, until a reversal occurs near 0.33 GPa. At higher pressures, the PL peak position shifts to the blue until PL vanishes above 2.5 GPa. We explain the pressure response with different modes of deformation of the perovskite crystal structure.



■ INTRODUCTION

Inorganic cesium lead halide perovskite nanocrystals (NCs), $CsPbX_3$ (X = Cl, Br, and I), have attracted much attention in recent years, following the pioneering synthetic work by Protesescu et al. Many groups have reported on different NC synthetic procedures, physical properties, and applications of the resulting NCs.^{2–10} Their composition-tunable, sharp absorption edges, and narrow photoluminescence (PL) spectra make them excellent candidates for next-generation lightemitting diode and photovoltaic (PV) applications. 1,5,11-14 Out of the family of CsPbX3 materials, CsPbI3 NCs, with their band gap at around 1.8 eV, show particular promise for applications in PV devices. For example, Swarnkar et al. have shown that a solar cell using a CsPbI3 NC film as the absorbing material can reach power conversion efficiencies of nearly 11%.5

Cesium lead halide perovskites belong to the family of ABX₃ perovskites, where A is a monovalent cation, B is a divalent metal cation, and X is a halide or oxygen ion. The ABX₃ perovskite crystal structure is composed of a network of cornersharing BX₆ octahedra, with the A cations occupying the cavities between the octahedra (Figure 1a). The bulk moduli of CsPbX₃ halides, which are a measure of the structural response of a material to pressure, have not been determined experimentally so far, with the exception of the nonperovskite δ-phase of CsPbI₃, which has a bulk modulus of 14 GPa. ¹⁵ The related organic/inorganic hybrid perovskite (CH₃NH₃)PbBr₃ has a bulk modulus of ca. 16 GPa, 16,17 placing it between soft molecular crystals, such as tetracene (ca. 9 GPa¹⁸), and harder semiconductor crystals, such as CdSe (ca. 53 GPa¹⁹). Given the relatively soft nature of metal halide perovskites, it is of interest to explore how perturbations to the crystal structure affect the optical gap of these materials. High pressure is a convenient

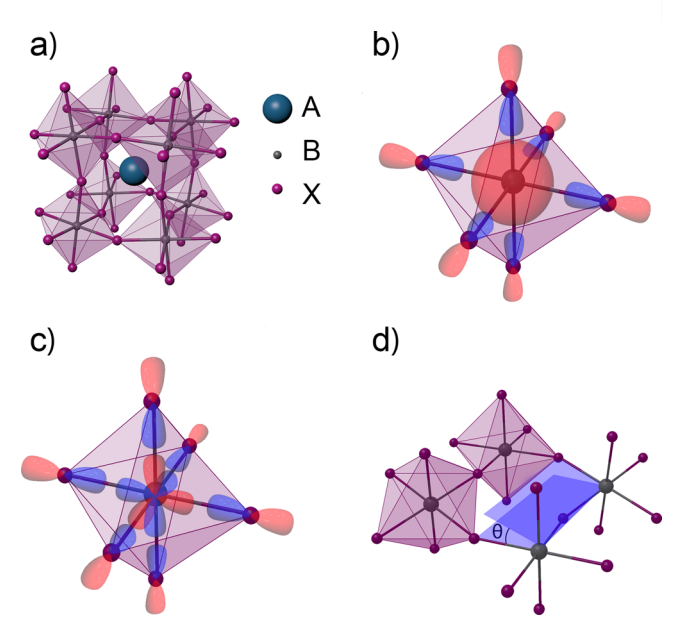


Figure 1. (a) Schematic of the *γ*-phase perovskite crystal structure. 33,34 (b) MOs generating the VBM. (c) MOs generating the CBM (d) tilting of the octahedra increases the dihedral angle θ which destabilizes the CBM,³⁵ causing a blue shift in the PL spectra (see text).

way to modify the structure of a condensed-phase sample by tuning interatomic distances, facilitating exploration of

Received: April 6, 2018 Revised: April 26, 2018 Published: April 27, 2018

[†]IILA, University of Colorado, Boulder, Colorado 80309-0440, United States

[‡]Department of Chemistry and Biochemistry, University of Colorado, Boulder, Colorado 80309-0215, United States

thermodynamics and structure, without increasing the thermal energy content or changing the chemical composition of the material. For lead halide perovskites, high-pressure techniques have been applied to bulk and NC samples of CsPbBr₃ $^{20-24}$ and (CH₃NH₃)PbX₃ (X = Cl, Br, and I)²⁵⁻³¹ as well as to bulk samples of CsPbCl₃, CH(NH₂)₂PbI₃, ³² and the nonperovskite, yellow phase of CsPbI₃. Is In the present work, we report a study of the pressure response of PL for CsPbI₃ NCs. We interpret our results with the aid of molecular orbital (MO) reasoning and using the similarity of the high-pressure response of CsPbI₃ with previously reported results on the pressure response of CsPbBr₃ NCs and bulk samples. ^{20,23}

METHODS

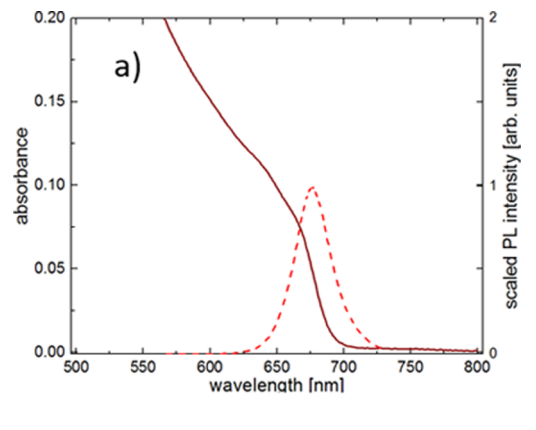
NC Synthesis, Sample Preparation, and Characterization. The NC synthesis was adapted form Wang et al. 10 and contains the following steps: a PbI₂ solution was prepared by adding 0.18 mmol PbI₂ (Aldrich, 99%), 5.0 mL of 1-octadecene (ODE) (Aldrich, technical grade, 90%), 0.5 mL of diisooctylphosphinic acid (DA) (Aldrich, technical grade, ~90%), and 0.5 mL of purified oleylamine (OA) 36 to a round-bottom flask. Water was removed using vacuum at 120 $^{\circ}$ C for 1 h with vigorous stirring.

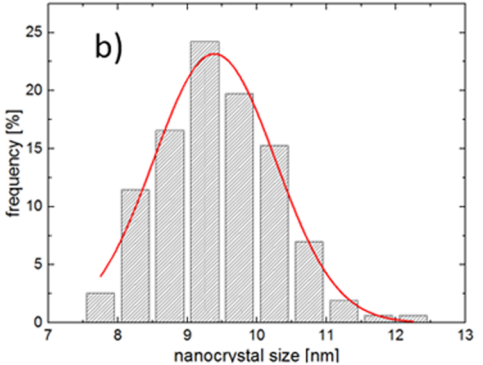
In a second round-bottom flask, we added 0.30 mmol Cs_2CO_3 (Aldrich, ReagentPlus, 99%), 5.0 mL of ODE, 0.5 mL of DA, and 0.5 mL of purified OA. This mixture was maintained at 120 °C under vacuum with vigorous stirring until all Cs_2CO_3 had dissolved and was then brought to 100 °C under dry nitrogen.

The PbI_2 solution was then brought to 140 °C under dry nitrogen. Next, 0.4 mL of the Cs_2CO_3 solution was injected into the PbI_2 solution with vigorous stirring and then immediately (within 5 s) transferred to a water bath. The resulting solution was washed by adding excess *tert*-butanol to precipitate NCs from the reaction mixture. This mixture was centrifuged at 6600 g, and the pellet was resuspended in anhydrous hexanes (Aldrich, \geq 99%) and stored at -21 °C. The samples obtained this way have a deep red/brown color and luminesce strongly in the red, in contrast to the nonemissive yellow phase, which we do not observe in our samples (see also Results and Discussion section).

To prepare the sample for high-pressure experiments, the NCs were dispersed in paraffin, which is hydrostatic over the pressure range studied in the present work, that is, up to ca. 3.0 GPa.³⁷ This was accomplished by adding equal amounts of paraffin oil to the hexane NC solution and then stirring under vacuum to remove the hexanes. The resulting solutions of NCs in paraffin were saturated.

The NCs have narrow PL spectra with full width at half-maximum of 30 nm and sharp band edge absorption (Figure 2a). The absorption spectra were acquired with a Cary 500 UV/vis spectrophotometer (resolution 2 nm, 10 mm path length). Although we were able to record UV/vis absorption spectra of the NC samples at ambient pressure, we had to use low concentrations because of the limited solubility of the NCs in paraffin. Combined with the very short optical path length in the diamond anvil cell (DAC) (70 μ m) and in the hydraulic pressure setup (50 μ m) as described below, these concentrations were too low to allow acquisition of absorption spectra under pressure. We note that CsPbBr₃ NCs exhibit much higher solubility and have indeed been studied by UV/vis absorption spectroscopy under pressure. ²³





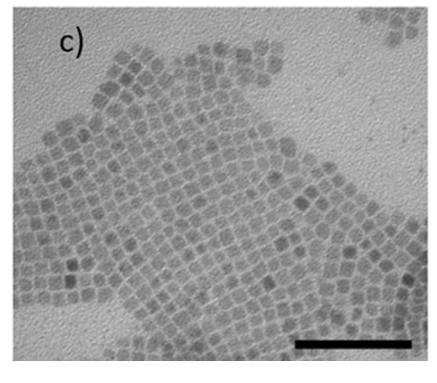


Figure 2. (a) Visible absorption (solid) and PL (dashed) spectra of CsPbI₃ NCs in hexanes. (b) Particle size distribution for CsPbI₃ NCs. (c) Example TEM image for size distribution. The scale bar is 100 nm.

Transmission electron microscopy (TEM) for size distribution analysis was performed using FEI Tecnai T12 Spirit at 120 keV. The samples contained highly monodisperse (9.8 \pm 2.0 nm) CsPbI $_3$ NCs (Figure 2b), which were used in the high-pressure experiments reported here. High-resolution TEM (HRTEM) images were taken using FEI Tecnai F20 at 200 keV and analyzed using ImageJ software.

Powder XRD patterns were taken on a Rigaku D/Max diffractometer using a Cu K α radiation source (λ = 0.1540562 nm). The patterns were recorded from 10° to 40° and acquired at a speed of 0.4°/min (Figure 3a).

High-Pressure Experiments. Two different setups were used for high pressure generation. The first setup is a gas membrane-driven DAC (easyLab Diacell μ ScopeDAC-RT(G), type Ia 16-sided diamond anvils, base diameter 2.5 mm, culet 0.50 mm, NA = 0.54). Blank high-pressure gaskets (type 302 stainless steel, initial thickness 250 μ m) were preindented to a final thickness of 90–100 μ m, and the sample compartment was formed by laser-drilling a hole with ca. 120 μ m diameter in

The Journal of Physical Chemistry C

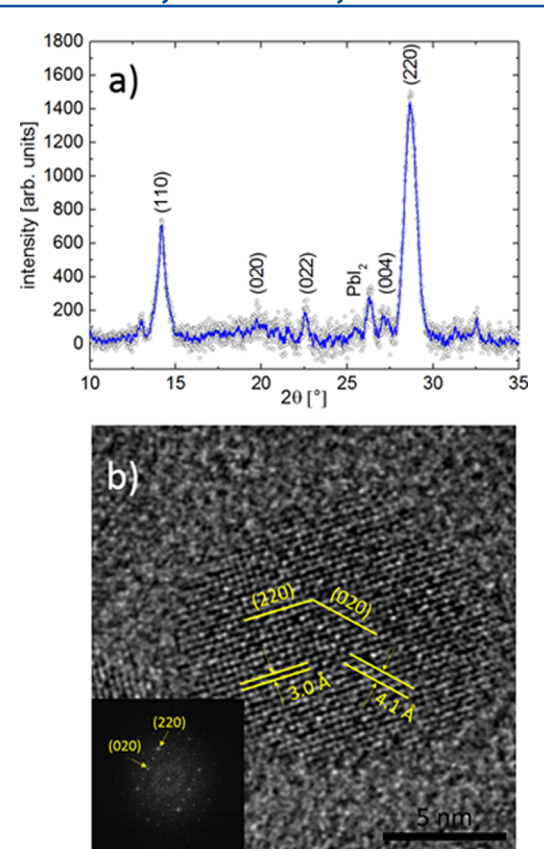


Figure 3. (a) XRD pattern of CsPbI₃ NCs. The light gray points are raw data; the solid blue line is a seven-point sliding average. The labeled peaks indicate that the NCs are in the perovskite orthorhombic phase as described in the most recent literature.^{3,33,44,45} (b) Sample HRTEM image of a CsPbI₃ NC and its Fourier transform, together with markers of the (020) and (220) planes.

the center of each preindented gasket. A small ruby grain was added to the cell along with a droplet of the sample, and the ruby R_1 fluorescence peak was used to determine the pressure, fitting the R_1 and R_2 lines with Lorentzian profiles. This method gives an error in our pressure measurements of 70 MPa 38

The CsPbI $_3$ samples were excited with a 532 nm continuous wave laser with intensities close to 100 W/cm 2 . The PL spectra did not change even under prolonged exposure and were the same as the spectra taken under much lower intensity, and we, therefore, judge that the irradiation caused no significant heating or photoinduced modification of the samples. All DAC spectra were recorded using a HORIBA Scientific XploRA confocal Raman microscope. The ruby fluorescence was measured using an 1800 lines/mm grating (0.1 nm resolution), whereas the NC PL spectra were acquired with a 600 lines/mm grating (0.3 nm resolution). The slit width of the monochromator was 50 μ m for all spectra. PL peaks were determined by fitting a Lorentzian to the observed spectra. The error of the PL peak energy associated with this procedure is based on the statistical uncertainty of the fit and amounts to ± 1 meV.

The second apparatus is a hydraulic pressure setup, modified from a design by Tekmen et al.,³⁹ with all components purchased from High Pressure Equipment Company (HIP, Erie, Pennsylvania). A hydraulic pressure generator (HIP, 25-5.75-100) capable of producing pressures as high as 700 MPa pressurized a set of stainless steel tubes filled with ethanol as

the pressure-transmitting fluid. The pressure was determined using a mechanical high pressure gauge (HIP, 6PG100). Perovskite NC samples were drawn into a quartz capillary with an outer diameter of 375 μ m and inner diameter of 50 μ m (Molex, TSU050375). A small amount of clean paraffin was then drawn into one end of the capillary to act as a barrier between the sample and ethanol in the high-pressure generating setup. The other end of the capillary was then fused using an oxygen/propane torch. The unfused end of the capillary was glued (Armstrong A-12 Epoxy) into a modified pressure plug (HIP, 100-7XM4), into which a 400 μ m hole had been drilled. The pressure plug was then coupled to the rest of the apparatus such that the unfused end of the capillary was in contact with ethanol in the pressure generating apparatus. In this setup, all samples were excited using a 532 nm laser with the confocal microscope.

CAUTION: In the hydraulic setup briefly described above, pressurization of glass or quartz capillaries may result in their destruction. If any gas bubbles are present in the apparatus, this can result in explosive release of pressure, which represents a hazard to people and equipment. Personal protective equipment must be worn at all times, and engineering solutions to prevent injury are strongly encouraged.

■ RESULTS AND DISCUSSION

Crystal Structure at Ambient Conditions. The exact perovskite polymorph that CsPbX₃ NCs adopt has been a point of debate in the literature for some time, as X-ray diffraction (XRD) and HRTEM data have been interpreted as evidence for cubic as well as orthorhombic perovskite crystal structures. ^{1,3,9,33} Therefore, the crystallographic analysis of the samples used in the present work merits further discussion.

Bulk CsPbI₃ is not stable in the perovskite crystal structure under ambient conditions, and multiple polymorphs exist at ambient pressure at different temperatures. The room-temperature phase has a nonperovskite crystal structure (yellow phase or δ -phase). Above room temperature, there are three distinct perovskite crystal structures, denoted α -, β -, and γ -CsPbI₃ with cubic, tetragonal, and orthorhombic crystal symmetries, respectively. The γ -CsPbI₃ phase is a direct band gap semiconductor with a band gap around 1.8 eV. S,41

In contrast to bulk, CsPbI₃ NCs are metastable as perovskite structures under ambient conditions. The assignment of crystal structure is complicated because nanocrystalline twins can exist in a single NC, which can lead to destructive interference of the diffraction signatures characteristic for the orthorhombic lattice. As a result, several accounts in the literature describe their samples as cubic, whereas others clearly identify CsPbI₃ NCs as orthorhombic. As permeated the literature, and even recent reports claim that their CsPbI₃ NCs are cubic. However, recent work by Bertolotti et al. has shown that CsPbI₃ NCs are in fact in the orthorhombic *Pnma* perovskite crystal structure under ambient conditions (γ -phase) and have been shown to retain this structure for long periods of time in NC and nanowire samples. γ -5,10,40–42

Powder XRD data indicate that our NC samples are in the orthorhombic γ -phase (Figure 3a) in agreement with the most recent literature. 3,10,33,43 We extract unit cell dimensions of a=8.6 Å, b=9.0 Å, and c=13.1 Å (error bars \pm 0.1 Å) from the XRD data, which are in good agreement with the reported values by Bertolotti et al. Using the Scherrer method to further analyze our XRD data, we found that the crystallite size was 10 ± 2 nm. This value is in agreement with the NC size

distribution we obtained from TEM image analysis, indicating that the NCs are single crystalline. The lattice spacings in the HRTEM images of CsPbI₃ NCs are consistent with the orthorhombic γ -phase assignment (Figure 3b). It is important to note that the orthorhombic γ -phase is not to be confused with the yellow δ -phase, which is also orthorhombic but does not have the perovskite structure and is not photoluminescent.

Pressure-Dependent PL. We measured the pressure-dependent shifts of the PL peak of our samples using hydrostatic pressures up to 3.0 GPa. We observed that the pressure response of the PL of CsPbI₃ NCs shows clear qualitative changes in behavior between different pressure regions. Figure 4 shows the PL spectra of CsPbI₃ NCs from a

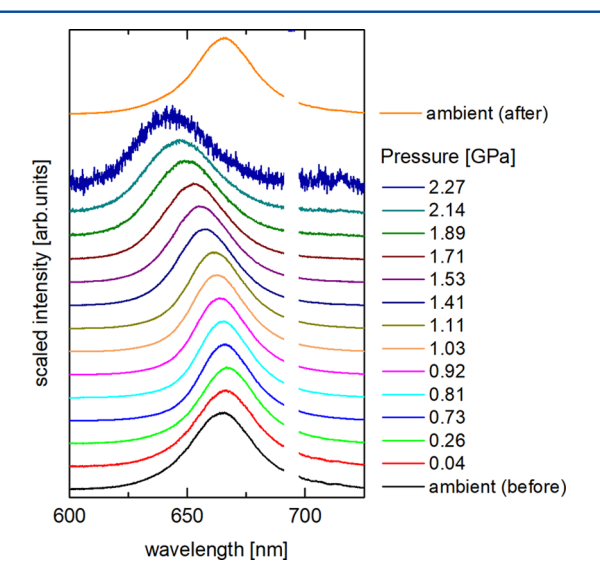


Figure 4. PL spectra of CsPbI₃ NCs at different pressures (right). All spectra are scaled to the same intensity. The ruby fluorescence peaks around 694 nm were deleted from the spectra for clarity (break in the spectra). The bottom and top traces show the PL spectra at ambient pressure before and after the pressure run.

typical DAC pressure run. At low pressures, the PL emission peak shifts slightly toward longer wavelengths, whereas it shifts to the blue at higher pressures. At ca. 2.3 GPa, the emission becomes very weak and finally disappears. Upon returning to ambient pressure, the PL emission returns in full, and the peak is observed at the same position as before pressurization.

Figure 5a shows the pressure response of CsPbI₃ NCs under hydrostatic pressure below 0.7 GPa, using the peak PL energy as a reference for the band gap $E_{\rm G}$. Upon initial compression, the energy of the PL maximum shifts to lower energies nearly linearly. We can approximately describe this behavior by

$$E_{\rm G} = E_0 + \alpha p \tag{1}$$

where E_0 is the ambient optical gap, and the pressure coefficient, α , describes the slope dE_G/dp . At low pressures, we find a pressure coefficient $\alpha = -14.0 \pm 0.6$ meV/GPa. This result is qualitatively similar to the behavior of CsPbBr₃, but the slope for CsPbBr₃ is much steeper, with α between -35 meV/GPa for bulk samples and -50 meV/GPa for NC samples at similar pressures. Further increase of pressure eventually leads to a change in the sign of α , resulting in a blue shift of the PL peak energy, beginning at ca 0.33 GPa and continuing up to 2.5 GPa (Figure 5). The change in the sign of the pressure

coefficient α is not accompanied by an observable drop in the PL intensity.

To explain this behavior, we consider the three different ways in which the perovskite crystal structure can respond to application of pressure: by compression of the MX_6 octahedra, by tilting of the octahedra, or by a phase transition into a different crystal structure. In the following, we will discuss how the first two different modes of deformation can be expected to affect the optical gap.

The band gap of bulk metal halide perovskites is at the Γ-point for orthorhombic structures. The valence band maximum (VBM) in CsPbI₃ perovskites arises from the antibonding interaction of Pb 6s and I 5p electronic orbitals (Figure 1b), 14,47,48 whereas the density of states at the conduction band minimum (CBM) is based primarily on the I 5p orbitals and Pb 6p orbitals (Figure 1c). 14,35,47,48 Although the small dimensions of the NCs do not allow the rigorous use of the bulk nomenclature for the symmetry points of the Brillouin zone, we expect that the overall character of the corresponding MO picture will be qualitatively similar.

Because the VBM at the Γ -point is dominated by antibonding interactions between the I 5p and Pb 6s orbitals, compression of the octahedra will result in destabilization of the VBM, pushing it to higher energies (see Figure 1b). The CBM is largely unaffected by octahedron compression because the net overlap of the I 5p and Pb 6p orbitals at the Γ -point gives the CBM a net nonbonding character (Figure 1c), and small changes in the Pb–I distance will not result in pronounced changes of the CBM energy. Therefore, the mode of deformation characterized by octahedron compression will result in the narrowing of the band gap and a concomitant red shift of the PL peak through the destabilization of the VBM, as observed in other perovskite materials. 20,23,25

Tilting of the octahedra (see Figure 1d) as a second mode of deformation will have the opposite effect. As shown by calculations by Amat et al., deviation of the Pb–I–Pb angle from 180° changes the mixing of Pb 6p and I 5p orbitals in the CBM and diminishes the contributions of Pb orbitals to the CBM. As a result, the impact of spin–orbit coupling on the CBM energy is lessened, and the CBM is destabilized. The net effect of tilting is a band gap increase and concomitant blue shift of the PL, consistent with the band gap change induced by varying the A cation and the accompanying change in the tilt angle θ between adjacent octahedra (see Figure 1d). degree θ

The overall behavior is very similar to that of CsPbBr₃ NCs, where these two modes of deformation were confirmed using in situ high-pressure powder XRD.²³ The above discussion explains the high-pressure behavior for both CsPbBr₃ and CsPbI₃ NCs. On the basis of the strong similarity between these two systems, we therefore interpret the observed red shift of the PL at low pressures as due to the compression of the Pb–I bonds. In analogy to CsPbBr₃,²³ we assign the change in the pressure response of the PL to a change in the mode of deformation from octahedron compression to octahedron tilting.

Different from the analogous case of CsPbBr₃ NCs, the change in the sign of α occurs near 0.33 GPa for CsPbI₃, much lower than the transition pressure for CsPbBr₃, which is close to 1.2 GPa. The earlier change in the mode of deformation can be qualitatively explained with the difference in the ionic radii of Br⁻ and I⁻. Because of the greater size of the iodide ions, the pressure at which octahedron compression bears a larger energy penalty than octahedron tilting, with the

The Journal of Physical Chemistry C

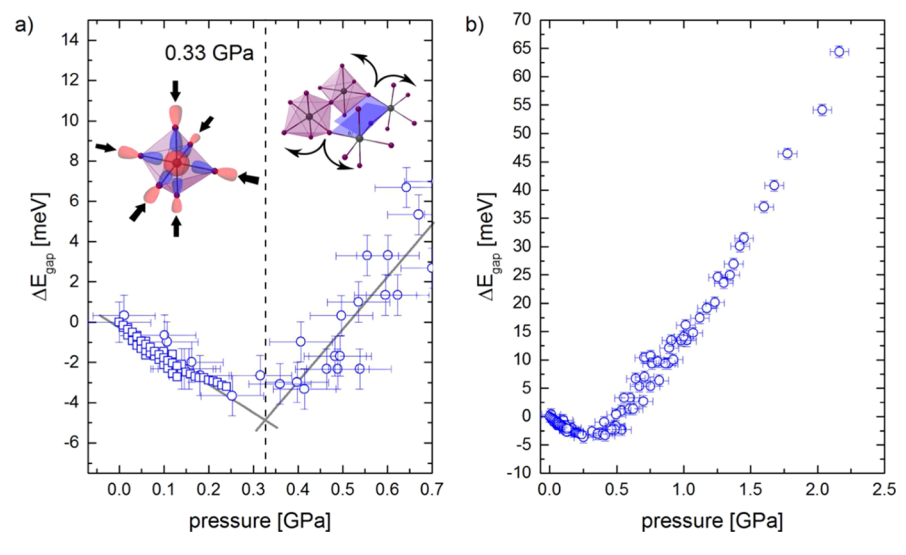


Figure 5. Pressure dependence of PL for CsPbI₃ NCs. The band gap energy change is plotted as the deviation of the PL peak at a given pressure from the ambient peak position. (a) Pressure range below 0.7 GPa. Data points from the hydraulic pressure generator (open squares) and data taken using the DAC (open circles) from several runs from each setup are shown. The gray lines indicate linear fits of the data in the two regions shown in this panel. The point at which they cross indicates the pressure where the mode of deformation changes (see text). (b) Overview of the entire pressure range up to 2.5 GPa, after which PL was no longer detected. Data from both the hydraulic pressure generator and the DAC are plotted together, and the data were obtained from several pressure runs. Error bars for the PL peak energy change are ±1 meV.

concomitant change in the mode of deformation, can be expected to be lower than that for bromide.

A second change in the pressure response of our samples occurs around 2.5 GPa, where the sample ceases to emit upon irradiation by 532 nm. This change is reversible upon release of pressure in the DAC and is likely to be the signature of a solidsolid phase transition, although the nature of the resulting highpressure phase is not clear at present. It is possible that this phase is the insulating nonperovskite δ -CsPbI₃ with an optical gap near 3.0 eV. This would explain the loss in PL under 532 nm irradiation as well as the reversibility becauseit has been shown in bulk CsPbI₃ that the δ -phase can be cycled back and forth with photoemitting perovskite phases by raising and lowering the temperature above and below 315 °C repeatedly. 49 Interestingly, the behavior observed for CsPbI₃ NCs is similar to that of bulk (CH3NH3)PbI3, which exhibits a phase transition at 0.26 GPa from tetragonal to orthorhombic and a second phase transition from orthorhombic to amorphous at 3 GPa.²⁸ The amorphous phase was much less emissive than the sample at ambient pressure (by a factor of 10⁻⁴).²⁸ Given this similarity, the dark phase in CsPbI₃ NCs could be amorphous. Alternatively, computational work on CsPbBr₃ predicts a phase transition at higher pressures associated with a change to an indirect band gap.²³ In light of these multiple possibilities, we refrain from a definitive assignment of the dark phase at present.

CONCLUSIONS

In summary, we have studied the pressure response of the PL peak position of $CsPbI_3$ NCs. The response to low hydrostatic pressure is characterized by the narrowing of the optical gap due to destabilization of the VBM. Near 0.33 GPa, the trend undergoes a transition because of a change in the mode of deformation that reverses of the sign of dE_G/dp . All pressure-induced changes in $CsPbI_3$ NCs are fully reversible in the pressure range up to 3.0 GPa. Together with the structural analysis of $CsPbI_3$ NCs at ambient pressure, we can draw the following conclusions from the pressure response of the PL:

- There is a close similarity between the structure and behavior of CsPbBr₃ and of CsPbI₃ NCs. Both are orthorhombic at ambient conditions, and both show qualitatively the same response to hydrostatic pressure. We therefore attribute the behavior of CsPbI₃ to the same mechanisms as found for CsPbBr₃ NCs;²³
- 2. At pressures below ca. 330 MPa, the behavior of the PL as a function of pressure is consistent with the compression of the PbI₆ octahedra as the active mode of deformation. Above this pressure, the PL behavior can be explained with an increased tilting of the octahedra;
- 3. The differences in the behavior between CsPbBr₃ and CsPbI₃ are based on the differences in the ionic radii of bromide and iodide. The larger radius of iodide causes the change in the dominant mode of deformation at much lower pressures for CsPbI₃ than that for CsPbBr₃; and
- 4. Around 2.5 GPa, CsPbI₃ NCs undergo a solid—solid phase transition to a nonemissive phase.

Future experiments on the pressure response of the optical properties of CsPbCl₃ NCs will be interesting, particularly because their structure has been identified as cubic, in contrast to the other two cesium lead halide perovskites.

AUTHOR INFORMATION

Corresponding Author

*E-mail: weberjm@jila.colorado.edu. Phone: ++1-303-492-7841.

ORCID ®

Gordana Dukovic: 0000-0001-5102-0958 J. Mathias Weber: 0000-0002-5493-5886

Present Address

[§]Department of Chemistry, Faculty of Science, Silpakorn University, Nakhon Pathom, 73000 Thailand.

Notes

The authors declare no competing financial interest.

ACKNOWLEDGMENTS

We thank Garry Morgan (University of Colorado at Boulder) for TEM facility services. J.M.W. and J.C.B. gratefully acknowledge the National Science Foundation for support through the JILA AMO Physics Frontier Center under Grant PHY-1734006. L.M.G.H., P.T., and G.D. acknowledge support from the Arnold and Mabel Beckman Foundation via the Beckman Young Investigator Award.

REFERENCES

- (1) Protesescu, L.; Yakunin, S.; Bodnarchuk, M. I.; Krieg, F.; Caputo, R.; Hendon, C. H.; Yang, R. X.; Walsh, A.; Kovalenko, M. V. Nanocrystals of Cesium Lead Halide Perovskites (CsPbX₃, X = Cl, Br, and I): Novel Optoelectronic Materials Showing Bright Emission with Wide Color Gamut. *Nano Lett.* **2015**, *15*, 3692–3696.
- (2) Wu, K.; Liang, G.; Shang, Q.; Ren, Y.; Kong, D.; Lian, T. Ultrafast Interfacial Electron and Hole Transfer from CsPbBr₃ Perovskite Quantum Dots. *J. Am. Chem. Soc.* **2015**, *137*, 12792–12795.
- (3) Cottingham, P.; Brutchey, R. L. On The Crystal Structure of Colloidally Prepared CsPbBr₃ Quantum Dots. *Chem. Commun.* **2016**, 52, 5246–5249.
- (4) Yettapu, G. R.; Talukdar, D.; Sarkar, S.; Swarnkar, A.; Nag, A.; Ghosh, P.; Mandal, P. Terahertz Conductivity within Colloidal CsPbBr₃ Perovskite Nanocrystals: Remarkably High Carrier Mobilities and Large Diffusion Lengths. *Nano Lett.* **2016**, *16*, 4838–4848.
- (5) Swarnkar, A.; Marshall, A. R.; Sanehira, E. M.; Chernomordik, B. D.; Moore, D. T.; Christians, J. A.; Chakrabarti, T.; Luther, J. M. Quantum Dot-Induced Phase Stabilization of α -CsPbI₃ Perovskite for High-Efficiency Photovoltaics. *Science* **2016**, *354*, 92–95.
- (6) Balakrishnan, S. K.; Kamat, P. V. Au–CsPbBr₃ Hybrid Architecture: Anchoring Gold Nanoparticles on Cubic Perovskite Nanocrystals. *ACS Energy Lett.* **2017**, *2*, 88–93.
- (7) Aneesh, J.; Swarnkar, A.; Ravi, V. K.; Sharma, R.; Nag, A.; Adarsh, K. V. Ultrafast Exciton Dynamics in Colloidal CsPbBr₃ Perovskite Nanocrystals: Biexciton Effect and Auger Recombination. *J. Phys. Chem. C* **2017**, *121*, 4734–4739.
- (8) Bekenstein, Y.; Koscher, B. A.; Eaton, S. W.; Yang, P.; Alivisatos, A. P. Highly Luminescent Colloidal Nanoplates of Perovskite Cesium Lead Halide and Their Oriented Assemblies. *J. Am. Chem. Soc.* **2015**, 137, 16008–16011.
- (9) Tong, Y.; Bladt, E.; Aygüler, M. F.; Manzi, A.; Milowska, K. Z.; Hintermayr, V. A.; Docampo, P.; Bals, S.; Urban, A. S.; Polavarapu, L.; et al. Highly Luminescent Cesium Lead Halide Perovskite Nanocrystals with Tunable Composition and Thickness by Ultrasonication. *Angew. Chem., Int. Ed.* **2016**, *55*, 13887–13892.
- (10) Wang, C.; Chesman, A. S. R.; Jasieniak, J. J. Stabilizing the Cubic Perovskite Phase of CsPbI₃ Nanocrystals by Using an Alkyl Phosphinic Acid. *Chem. Commun.* **2016**, *53*, 232–235.
- (11) Huang, H.; Polavarapu, L.; Sichert, J. A.; Susha, A. S.; Urban, A. S.; Rogach, A. L. Colloidal Lead Halide Perovskite Nanocrystals: Synthesis, Optical Properties and Applications. NPG Asia Mater. 2016, 8, 1–15.
- (12) Swarnkar, A.; Chulliyil, R.; Ravi, V. K.; Irfanullah, M.; Chowdhury, A.; Nag, A. Colloidal CsPbBr₃ Perovskite Nanocrystals: Luminescence beyond Traditional Quantum Dots. *Angew. Chem., Int. Ed.* **2015**, 127, 15644–15648.
- (13) Sutherland, B. R.; Sargent, E. H. Perovskite Photonic Sources. *Nat. Photonics* **2016**, *10*, 295.
- (14) Manser, J. S.; Christians, J. A.; Kamat, P. V. Intriguing Optoelectronic Properties of Metal Halide Perovskites. *Chem. Rev.* **2016**, *116*, 12956–13008.
- (15) Yuan, G.; Qin, S.; Wu, X.; Ding, H.; Lu, A. Pressure-Induced Phase Transformation of CsPbI₃ by X-Ray Diffraction and Raman Spectroscopy. *Phase Transitions* **2018**, *91*, 38–47.
- (16) Rakita, Y.; Cohen, S. R.; Kedem, N. K.; Hodes, G.; Cahen, D. Mechanical Properties of APbX₃ (A = Cs or CH₃NH₃; X = I or Br) Perovskite Single Crystals. MRS Commun. 2015, 5, 623–629.

- (17) Lomonosov, A. M.; Yan, X.; Sheng, C.; Gusev, V. E.; Ni, C.; Shen, Z. Exceptional Elastic Anisotropy of Hybrid Organic-Inorganic Perovskite CH₃NH₃PbBr₃ Measured by Laser Ultrasonic Technique. *Phys. Status Solidi* **2016**, *10*, 606–612.
- (18) Oehzelt, M.; Aichholzer, A.; Resel, R.; Heimel, G.; Venuti, E.; Della Valle, R. G. Crystal Structure of Oligoacenes Under High Pressure. *Phys. Rev. B: Condens. Matter Mater. Phys.* **2006**, *74*, 104103.
- (19) Strauch, D. Semiconductors; Springer-Verlag: Berlin, 1991.
- (20) Zhang, L.; Zeng, Q.; Wang, K. Pressure-Induced Structural and Optical Properties of Inorganic Halide Perovskite CsPbBr₃. *J. Phys. Chem. Lett.* **2017**, *8*, 3752–3758.
- (21) Gesi, K.; Ozawa, K.; Hirotsu, S. Effect of Hydrostatic Pressure on the Structural Phase Transitions in CsPbCl₃ and CsPbBr₃. *J. Phys. Soc. Jpn.* **1975**, *38*, 463–466.
- (22) Hirotsu, S.; Harada, J.; Iizumi, M.; Gesi, K. Structural Phase Transitions in CsPbBr₃. *J. Phys. Soc. Jpn.* **1974**, *37*, 1393–1398.
- (23) Xiao, G.; Cao, Y.; Qi, G.; Wang, L.; Liu, C.; Ma, Z.; Yang, X.; Sui, Y.; Zheng, W.; Zou, B. Pressure Effects on Structure and Optical Properties in Cesium Lead Bromide Perovskite Nanocrystals. *J. Am. Chem. Soc.* **2017**, *139*, 10087–10094.
- (24) Nagaoka, Y.; Hills-Kimball, K.; Tan, R.; Li, R.; Wang, Z.; Chen, O. Nanocube Superlattices of Cesium Lead Bromide Perovskites and Pressure-Induced Phase Transformations at Atomic and Mesoscale Levels. *Adv. Mater.* **2017**, *29*, 1606666.
- (25) Wang, L.; Wang, K.; Xiao, G.; Zeng, Q.; Zou, B. Pressure-Induced Structural Evolution and Band Gap Shifts of Organometal Halide Perovskite-Based Methylammonium Lead Chloride. *J. Phys. Chem. Lett.* **2016**, *7*, 5273–5279.
- (26) Szafrański, M.; Katrusiak, A. Photovoltaic Hybrid Perovskites Under Pressure. *J. Phys. Chem. Lett.* **2017**, *8*, 2496–2506.
- (27) Xiao, J.; Yang, Y.; Xu, X.; Shi, J.; Zhu, L.; Lv, S.; Wu, H.; Luo, Y.; Li, D.; Meng, Q. Pressure-Assisted CH₃NH₃PbI₃ Morphology Reconstruction to Improve the High Performance of Perovskite Solar Cells. *J. Mater. Chem. A* **2015**, *3*, 5289–5293.
- (28) Capitani, F.; Marini, C.; Caramazza, S.; Postorino, P.; Garbarino, G.; Hanfland, M.; Pisanu, A.; Quadrelli, P.; Malavasi, L. High-Pressure Behavior of Methylammonium Lead Iodide (MAPbI₃) Hybrid Perovskite. *J. Appl. Phys.* **2016**, *119*, 185901.
- (29) Matsuishi, K.; Ishihara, T.; Onari, S.; Chang, Y. H.; Park, C. H. Optical Properties and Structural Phase Transitions of Lead-Halide Based Inorganic—Organic 3D and 2D Perovskite Semiconductors Under High Pressure. *Phys. Status Solidi B* **2004**, 241, 3328—3333.
- (30) Yin, T.; Fang, Y.; Chong, W. K.; Ming, K. T.; Jiang, S.; Li, X.; Kuo, J.-L.; Fang, J.; Sum, T. C.; White, T. J.; et al. High-Pressure-Induced Comminution and Recrystallization of CH₃NH₃PbBr₃ Nanocrystals as Large Thin Nanoplates. *Adv. Mater.* **2018**, 30, 1705017.
- (31) Jaffe, A.; Lin, Y.; Beavers, C. M.; Voss, J.; Mao, W. L.; Karunadasa, H. I. High-Pressure Single-Crystal Structures of 3D Lead-Halide Hybrid Perovskites and Pressure Effects on their Electronic and Optical Properties. *ACS Cent. Sci.* **2016**, *2*, 201–209.
- (32) Wang, P.; Guan, J.; Galeschuk, D. T. K.; Yao, Y.; He, C. F.; Jiang, S.; Zhang, S.; Liu, Y.; Jin, M.; Jin, C.; et al. Pressure-Induced Polymorphic, Optical, and Electronic Transitions of Formamidinium Lead Iodide Perovskite. *J. Phys. Chem. Lett.* **2017**, *8*, 2119–2125.
- (33) Bertolotti, F.; Protesescu, L.; Kovalenko, M. V.; Yakunin, S.; Cervellino, A.; Billinge, S. J. L.; Terban, M. W.; Pedersen, J. S.; Masciocchi, N.; Guagliardi, A. Coherent Nanotwins and Dynamic Disorder in Cesium Lead Halide Perovskite Nanocrystals. *ACS Nano* **2017**, *11*, 3819–3831.
- (34) Persson, K. Materials Data on CsPbBr3 (SG:62) by Materials Project; United States. Department of Energy. Office of Basic Energy Sciences: United States, 2014.
- (35) Amat, A.; Mosconi, E.; Ronca, E.; Quarti, C.; Umari, P.; Nazeeruddin, M. K.; Grätzel, M.; De Angelis, F. Cation-Induced Band-Gap Tuning in Organohalide Perovskites: Interplay of Spin—Orbit Coupling and Octahedra Tilting. *Nano Lett.* **2014**, *14*, 3608–3616.

- (36) Baranov, D. Synthesis of Lead Sulfide Nanocrystals and Their Two-Dimensional Electronic Spectra in a Spinning Cell. Ph.D. Thesis, University of Colorado, May 2017.
- (37) Otto, J. W.; Vassiliou, J. K.; Frommeyer, G. Nonhydrostatic Compression of Elastically Anisotropic Polycrystals. I. Hydrostatic Limits of 4:1 Methanol-Ethanol and Paraffin Oil. Compression of Elastically Anisotropic Polycrystals. I. Hydrostatic Limits of 4:1 Methanol-Ethanol and Paraffin Oil 1998, 57, 3253–3263.
- (38) Holzapfel, W. B. Refinement of the Ruby Luminescence Pressure Scale. *J. Appl. Phys.* **2003**, *93*, 1813–1818.
- (39) Tekmen, M.; Müller, J. D. High-Pressure Cell for Fluorescence Fluctuation Spectroscopy. *Rev. Sci. Instrum.* **2004**, *75*, 5143–5148.
- (40) Stoumpos, C. C.; Kanatzidis, M. G. The Renaissance of Halide Perovskites and Their Evolution as Emerging Semiconductors. *Acc. Chem. Res.* **2015**, *48*, 2791–2802.
- (41) Kondo, S.; Masaki, A.; Saito, T.; Asada, H. Fundamental Optical Absorption of CsPbI₃ and Cs₄PbI₆. Solid State Commun. **2002**, 124, 211–214.
- (42) Lai, M.; Kong, Q.; Bischak, C. G.; Yu, Y.; Dou, L.; Eaton, S. W.; Ginsberg, N. S.; Yang, P. Structural, Optical, and Electrical Properties of Phase-Controlled Cesium Lead Iodide Nanowires. *Nano Res.* **2017**, *10*, 1107–1114.
- (43) Udayabhaskararao, T.; Houben, L.; Cohen, H.; Menahem, M.; Pinkas, I.; Avram, L.; Wolf, T.; Teitelboim, A.; Leskes, M.; Yaffe, O.; et al. A Mechanistic Study of Phase Transformation in Perovskite Nanocrystals Driven by Ligand Passivation. *Chem. Mater.* **2017**, *30*, 84–93.
- (44) Eaton, S. W.; Lai, M.; Gibson, N. A.; Wong, A. B.; Dou, L.; Ma, J.; Wang, L.-W.; Leone, S. R.; Yang, P. Lasing in Robust Cesium Lead Halide Perovskite Nanowires. *Proc. Natl. Acad. Sci. U.S.A.* **2016**, *113*, 1993–1998.
- (45) Li, G.; Wang, H.; Zhu, Z.; Chang, Y.; Zhang, T.; Song, Z.; Jiang, Y. Shape and Phase Evolution from CsPbBr₃ Perovskite Nanocubes to Tetragonal CsPb₂Br₅ Nanosheets with an Indirect Bandgap. *Chem. Commun.* **2016**, *52*, 11296–11299.
- (46) Angel, R. J.; Zhao, J.; Ross, N. L. General Rules for Predicting Phase Transitions in Perovskites Due to Octahedral Tilting. *Phys. Rev. Lett.* **2005**, *95*, 025503.
- (47) Borriello, I.; Cantele, G.; Ninno, D. Ab initio Investigation of Hybrid Organic-Inorganic Perovskites Based on Tin Halides. *Ab initio Investigation of Hybrid Organic-Inorganic Perovskites Based on Tin* **2008**, 77, 235214.
- (48) Fröhlich, D.; Heidrich, K.; Künzel, H.; Trendel, G.; Treusch, J. Cesium-Trihalogen-Plumbates a New Class of Ionic Semiconductors. *J. Lumin.* **1979**, *18*, 385–388.
- (49) Eperon, G. E.; Paternò, G. M.; Sutton, R. J.; Zampetti, A.; Haghighirad, A. A.; Cacialli, F.; Snaith, H. J. Inorganic Caesium Lead Iodide Perovskite Solar Cells. *J. Mater. Chem. A* **2015**, 3, 19688–19695.